

Characteristics of gravitationally affected colloidal plasma sheath

Kavita Rani Rajkhowa and H. Ramachandran

Citation: *Physics of Plasmas* (1994-present) **11**, 1203 (2004); doi: 10.1063/1.1645521

View online: <http://dx.doi.org/10.1063/1.1645521>

View Table of Contents: <http://scitation.aip.org/content/aip/journal/pop/11/3?ver=pdfcov>

Published by the [AIP Publishing](#)

Articles you may be interested in

[Fluid simulation of an electrostatic plasma sheath with two species of positive ions and charged nanoparticles](#)
Phys. Plasmas **17**, 123711 (2010); 10.1063/1.3527991

[Structure of the magnetized sheath of a dusty plasma](#)
Phys. Plasmas **17**, 123708 (2010); 10.1063/1.3526740

[Simulation of the collisional sheath structure near the outer wall of the Hall thruster](#)
Phys. Plasmas **12**, 033506 (2005); 10.1063/1.1850478

[Dynamic behaviors of dust particles in the plasma–sheath boundary](#)
Phys. Plasmas **8**, 1886 (2001); 10.1063/1.1350967

[Dust-plasma sheath: A new dissipative self-organized structure](#)
Phys. Plasmas **6**, 2972 (1999); 10.1063/1.873596



Vacuum Solutions from a Single Source

- Turbopumps
- Backing pumps
- Leak detectors
- Measurement and analysis equipment
- Chambers and components

PFEIFFER  **VACUUM**

Characteristics of gravitationally affected colloidal plasma sheath

Kavita Rani Rajkhowa

Centre of Plasma Physics, Dispur, Guwahati-781 006, India

H. Ramachandran

Department of Electrical Engineering, IIT Madras, Chennai-600 036, India

(Received 23 September 2003; accepted 8 December 2003)

The presence of massive dust grains modifies the flow structures of plasma species in presheath and sheath regions as well as the nature of boundary conditions at the sheath edge. The work presents a one-dimensional approach to study the plasma sheath profiles in the presheath and sheath regions of a colloidal plasma. Electrons are assumed to be Boltzmannian and ions and dusts are assumed to be adiabatic fluid with finite temperature in the absence of a source. The set of equations is solved numerically for the presheath and the sheath regions to explore the possible physical solutions. Solutions for presheath and sheath regions in continuity are obtained. Combined effects of electrostatic, neutral drag, and external gravity forces are included to analyze the solutions for three distinct cases for both interacting and noninteracting dust. The likely existence of levitational equilibrium is explored. © 2004 American Institute of Physics. [DOI: 10.1063/1.1645521]

I. INTRODUCTION

There has been a recent increase in interest in low temperature plasma with dust, commonly referred to as “colloidal plasmas”¹ or the “dusty plasmas.”² Colloidal plasmas are frequently observed in many practical situations of interest ranging from astrophysical to laboratory plasmas. The theory of plasma near the boundary wall region containing several species of ions is of importance for various branches of plasma physics and plasma technology ranging from gas discharge lamps, gas lasers, plasma–surface interactions,^{3–6} controlled nuclear fusion,^{7,8} and astrophysics.^{9,10} It is thus of practical interest to investigate the interaction between a colloidal plasma and a solid boundary.

The study of dust levitating in terrestrial sheaths, especially in so-called plasma crystals, has been underway since 1994, when Chu *et al.*¹¹ and Thomas *et al.*¹² experimentally produced such crystals. Dust particles have been observed at the plasma-sheath boundary in etching,^{13,14} deposition,¹⁵ and sputter plasmas.¹⁶ These microparticles result from sputtering of the electrode and wall surfaces, gas phase nucleation and polymerization. This results in contamination in plasma processing of integrated circuits. Plasma dust has been identified as a serious barrier to maximizing product yields. The dust particles can be observed directly using laser scattering techniques.¹⁵ The experimental observation of the microparticles or the dust grains has shown that these particles are trapped close to the plasma-sheath boundary¹³ near the electrodes or at the other near-wall regions.^{3,4} Due to their electrical nature the dust grains tend to congregate into particle traps also referred to as electrostatic traps.¹⁷ The dust grains in the traps are negatively charged and thus their suspension locations are mainly determined by the electrical field experienced by the dust grains near the boundary surface. Besides the electrostatic force, many other forces like gravitational and drag forces, also affect the particle suspension and motion.

The study of plasma sheath in colloidal plasmas under various forces has been done since the early 1990s.^{18,19} The electrostatic sheath of dusty plasmas has been studied for dynamic and stationary dust grains under both the constant and variable charge models.^{20–22} Existing theoretical studies of the dusty plasma sheath have been based on investigations of dynamics of dust grains and its impact on the sheath electric field and the dynamics of plasma species under different model systems.

The dust particles can significantly influence sheath properties due to their continuous interaction with background electrons and ions, which can cause an essential change of both electron and ion distribution as well as the ion flux entering the sheath. As a result, spatial distributions of plasma parameters in sheaths can be significantly changed including the potential profile, which determine the properties of dust oscillations and waves in sheaths.

The aim of this work is to study the characteristics of the plasma sheath in colloidal plasmas under the effect of electrostatic, gravitational, and drag forces. The influence of dust grains on all the parameters of the sheath, in particular, the electric field distributions and the flow velocities of plasma particles under the combined effect of electrostatic, gravitational, and drag forces is studied. Previously, various models of dust in the low temperature plasma discharge sheath region were numerically considered.^{20–22} But the investigations were confined to the solution of the Poisson’s equation in the sheath region only. In this paper we demonstrate a new approach to study the dynamics of the gravitationally sensitive colloidal plasmas in both the presheath and the sheath regions. Solutions for both interacting and noninteracting dust grains are studied.

The organization of this paper is as follows: In Sec. II the model system of the plasma and the governing equations are discussed. Section III describes in detail the charging of dust grains. Section IV discusses the mathematical formula-

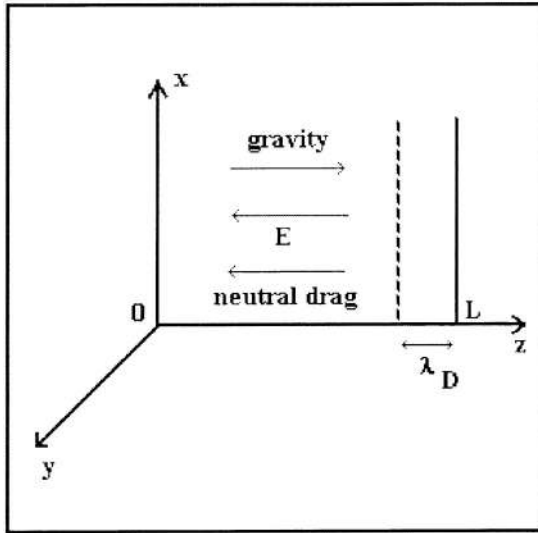


FIG. 1. Model system under consideration. $z=0$ defines the beginning of the presheath and $z=L$ is the position of the wall.

tion of the presheath and the sheath regions. The solution procedure is discussed in Sec. V. Section VI describes in detail the results and conclusions are given in Sec. VII.

II. MODEL PLASMA SYSTEM

The model plasma under consideration is shown in Fig. 1. The plasma sheath and presheath are assumed to be confined to $0 < z < L$. The bulk collisional plasma present in $z < 0$ is assumed to be large enough in extent that the dust particles have reached their terminal velocities before entering the presheath. The source of dust particles is assumed to be some point in $z < 0$. The presheath is assumed to be free of dust sources.

The following assumptions have been used to obtain the model equations derived in this section.

A steady state one-dimensional plasma model is considered. No source is present. No magnetic fields are present. Dust grains are assumed to have same mass (m_I) and size (a) and are spherically symmetric. The charge on the dust grains is determined self-consistently by the plasma currents collected at the grain.

The model plasma under consideration is a weakly ionized plasma. Thus, the collision between the charged particles and the neutrals are abundant. These short-range encounters of (ionized) plasma particles with the neutral background, ion-neutral collision ν_{in} and dust neutral collision ν_{In} , dominates and determine the transport properties of the plasma like diffusion, conductivity, etc. In this analysis, collisions of plasma particles with neutral particles is modelled as a drag, with ion and neutral temperatures being equal due to frequent collisions. The neutrals absorb all the energy received due to impact of ions and dust. However, they are assumed to be so numerous that their temperature and flow velocity remain constant.

A simple plane sheath model under the combined effect of gravitational force, electrostatic force, and collisional drag force is considered. The gravitational force acts along the

direction of the wall and the electrostatic force acts in opposite direction. The walls are assumed to be ideal, i.e., there is no secondary emission from the wall. It is also assumed that the source of dust and ions is in the “bulk.” Ions are neither created nor neutralized in the presheath.

Governing equations: The basic set of equations are as follows.

Electrons are assumed to be Boltzmannian, i.e., inertialess, with the electron pressure balancing the electrostatic forces. The electrons are assumed to be isothermal. There is no momentum loss of electrons to neutrals,

$$(-e) \frac{d\phi}{dz} = -\frac{T_e}{n_e} \frac{dn_e}{dz}, \quad (1)$$

where n_e and T_e represents the density and temperature of the electrons.

The ions are treated as an adiabatic fluid and the dynamics of the ion are described by the continuity and the momentum equations. The steady state continuity equation simply conserves ions due to the absence of an ion source,

$$n_i v_i = n_{i0} v_{i0}. \quad (2)$$

The momentum equation is the standard presheath equation for ions, with a friction term added. However, it should be noted that $n_e \neq n_i$ in such a system. The ions are assumed to be adiabatic inside the presheath, i.e., $\gamma_i = 3$,

$$m_i v_i \frac{dv_i}{dz} = -e \frac{d\phi}{dz} - \frac{\gamma_i T_i}{n_i} \frac{dn_i}{dz} - m_i \nu_{in} v_i, \quad (3)$$

where m_i , n_i , and v_i represents the mass, density, and flow velocity of ions, respectively. ν_{in} is the ion-neutral collision frequency and T_i is the ion temperature. The assumption of adiabatic ions is not consistent with ion-neutral drag. A more correct energy equation could be derived that takes ion-neutral collisions into account. However, in this analysis, we have made the simplifying assumption that in the region where $T_i \neq T_0$ matters (the end of the presheath and the sheath), the variation of T_i occurs on scale lengths that are much shorter than λ_{mfp} .

The dust particles also satisfy the continuity and momentum equations. The dust continuity equation is given by conservation of dust particles in the absence of a local source of dust,

$$n_I v_I = n_{I0} v_{I0}. \quad (4)$$

The dust momentum equation is like the ion momentum equation, Eq. (3), with a gravitational term added. The adiabatic equation of state has again been used to close the moments with $\gamma_I = 3$. The reason for this is that while the dust is very collisional with itself (i.e., it evolves quasistatically), it is not able to exchange energy efficiently with the neutrals. The momentum equation does not include the term representing frictional drag between the dust and the ions. This term is assumed to be negligible in a weakly ionized plasma, but could be taken into account without difficulty,

$$m_I v_I \frac{dv_I}{dz} = -Z_I e \frac{d\phi}{dz} - \frac{\gamma_I T_I}{n_I} \frac{dn_I}{dz} + m_I g_E - m_I \nu_{In} v_I. \quad (5)$$

Here, n_I, v_I, m_I, T_I defines the density, flow velocity, mass, and temperature of the dust grains. ν_{In} is the dust-neutral collision frequency and g_E is the external gravity. Subscript “ I ” denotes the “impurity ions” in general.

These equations are closed by the Poisson’s equation,

$$\frac{d^2\phi}{dz^2} = 4\pi e[n_e - n_i - Z_I n_I]. \tag{6}$$

The consideration of adiabatic and collisional dynamics of ions and dust grains is different from the earlier analysis by some of the authors,^{20,22} where the ions are considered as cold fluid and the electrostatic and gravitational forces dominate the dynamics of the dust grains.

III. CHARGE ON DUST GRAINS

In this analysis, dust grains are considered to be isolated, i.e., $a \ll \lambda_D \ll d$, where d is the intergrain distance. This means that particle–particle interactions which reduce the charge on the particle can be ignored. The charge on the dust grain is calculated by estimating the potential difference between the dust particle and the plasma using the orbit-motion limited (OML) probe theory developed by Mott-Smith and Langmuir.²³ The electrons are assumed to be in thermal equilibrium and the thermal electron current to the dust particle is given by

$$I_e = -4\pi a^2 e n_e \left(\frac{k_B T_e}{2\pi m_e}\right)^{1/2} \exp\left(\frac{e\phi_I}{k_B T_e}\right), \tag{7}$$

where k_B is the Boltzmann constant, ϕ_I is the dust surface potential, m_e is the electronic mass, e is the electronic charge.

Ion current velocities in the bulk plasma are typically less than the ion thermal velocity. The ion current reaching the dust particle surface is then given by

$$I_i = 4\pi a^2 e n_i \left(\frac{k_B T_i}{2\pi m_i}\right)^{1/2} \left(1 - \frac{e\phi_I}{k_B T_i}\right) \tag{8}$$

for a random thermal ion current with a Maxwellian velocity distribution in the orbit motion limit.

In a more general case, like in the case of colloidal plasma, the situation may arise in which the ions have some finite streaming velocity. Such a situation is typical for a dust particle in the proximity of a boundary wall. In such a case the ion current collected at the dust surface is due to the monoenergetic ions directed towards the wall with finite velocity much larger than the ion thermal speed. Then ion current to the dust grains can be approximately written as below,

$$I_i = \pi a^2 e n_i v_i \left(1 - \frac{2e\phi_I}{m_i v_i^2}\right). \tag{9}$$

This represents a unidirectional current which charged the particle, rather than a spherically symmetric current, hence the particle cross-sectional area rather than the surface area is used. “ v_i ” is the streaming velocity of ions.

This paper presents the solution in both the presheath and the sheath region. The ion dynamics are described differently on two different scales, presheath and sheath. In the

presheath limit, the ions are described by the Maxwellian distribution and thus, the thermal dynamics dominate [Eq. (8)]. Whereas in the other limit, i.e., the region near the sheath, the ions have supersonic streaming speed and the expression for the current is given by Eq. (9). Thus, there is a need to formulate a single equation for the ion current which is valid in both the limits. In order to do so, we combined Eqs. (8) and (9) to write in the form written below,

$$I_i = \pi a^2 e n_i \left(v_i^2 + \frac{8k_B T_i}{\pi m_i}\right)^{1/2} \left(1 - \frac{e\phi_I}{\left(k_B T_i + \frac{1}{2} m_i v_i^2\right)}\right). \tag{10}$$

Therefore, for low directed ion velocity, the above Eq. (10) is in the thermal limit and resembles Eq. (8). Alternatively, when the velocity is high, the ion current Eq. (10) is in the monoenergetic beam limit and resembles Eq. (9).

The potential difference between the dust particle and the plasma, ϕ_I is calculated by equating the ion current to the electron current which is analogous to the calculation of the floating potential on a collecting spherical probe in the orbit-motion-limited regime.

The charge on the dust grain, Q_I , is estimated using basic electrostatic theory for a charged, conducting sphere with the zero reference at infinity, it is given by

$$Q_I = 4\pi \epsilon_0 a \phi_I. \tag{11}$$

The expression for potential for floating condition, $I_e = I_i$, is then written as

$$\psi_I = -\ln\left[\frac{\frac{N_e}{N_i}}{P(1 - \beta\psi_I)}\right], \tag{12}$$

where

$$P = \left(\frac{T_i}{T_e} \frac{m_e}{m_i}\right)^{1/2} \left(1 + \frac{\pi M_i^2 T_e}{8 T_i}\right)^{1/2}, \quad \beta = \left[1/\left(\frac{T_i}{T_e} + \frac{M_i^2}{2}\right)\right], \tag{13}$$

N_e and N_i are the density of electrons and ions normalized to their equilibrium value respectively. $M_i = v_i/c_s$, $c_s = \sqrt{k_B T_e/m_i}$ and $\psi_I = e\phi_I/k_B T_e$. Thus, the expression to calculate charge on dust can be written as

$$Q_I = \lambda \psi_I,$$

where

$$\lambda = \frac{4\pi \epsilon_0 a T_e}{e^2}. \tag{14}$$

IV. MATHEMATICAL FORMULATION

In steady state, the one-dimensional fluid Eqs. (1)–(6) govern the dynamics of different species, electrons, ions, and dust grains. In order to determine the solutions, these equations can be written in dimensionless form as follows:

$$\frac{d\psi}{d\xi} = -\frac{1}{N_e} \frac{dN_e}{d\xi}, \tag{15}$$

$$N_i = M_{i0} M_i^{-1}, \quad (16)$$

$$M_i \frac{dM_i}{d\xi} = \frac{d\psi}{d\xi} - \gamma_i \frac{T_i}{T_e} \frac{1}{N_i} \frac{dN_i}{d\xi} - \hat{v}_{in} M_i, \quad (17)$$

$$N_I = M_{I0} M_I^{-1}, \quad (18)$$

$$M_I \frac{dM_I}{d\xi} = Z_I \frac{m_i}{m_I} \frac{d\psi}{d\xi} - \gamma_I \frac{T_I}{T_e} \frac{m_i}{m_I} \frac{1}{N_I} \frac{dN_I}{d\xi} + \hat{g}_E - \hat{v}_{In} M_I, \quad (19)$$

$$\left(\frac{\lambda_{De}}{L}\right)^2 \frac{d^2\psi}{d\xi^2} = [N_i + \epsilon_I N_I - N_e], \quad (20)$$

where the normalizations used are as follows:

$$\psi = -\frac{e\phi}{k_B T_e}, \quad \xi = \frac{z}{L}, \quad M_i = \frac{v_i}{c_s}, \quad M_{i0} = \frac{v_{i0}}{c_s},$$

$$M_I = \frac{v_I}{c_s}, \quad M_{I0} = \frac{v_{I0}}{c_s}, \quad c_s = \sqrt{\frac{k_B T_e}{m_i}}, \quad \hat{g}_E = \frac{g_E L}{c_s^2}, \quad (21)$$

$$\hat{v}_{in} = \frac{v_{in} L}{c_s}, \quad \hat{v}_{In} = \frac{v_{In} L}{c_s}, \quad \epsilon_I = Z_I \frac{n_{I0}}{n_{e0}},$$

$$N_j = \frac{n_j}{n_{j0}}, \quad j = e, i, I.$$

The space coordinate is normalized by a generalized scale. The dimension L of the system is large compared to the Debye length λ_{De} . The study of plasma sheath is usually based on a two scale analysis. And it is evident from literature, in the asymptotic limit $\lambda_D/L \rightarrow 0$, the hydrodynamic description of a bounded plasma leads to singularities and requires special numerical and analytical treatment for smooth solutions. The formulation for the quasineutral presheath and the space charge dominated sheath is discussed below.

A. Presheath region

The presheath region is described by the scale length $L = \lambda_{mfp}$, where λ_{mfp} is the last mean free path of the ions. Thus, on the presheath scale $\xi = z/L = z/\lambda_{mfp}$. It is assumed that λ_{mfp} is large compared to the Debye length (λ_{De}) (collisionless sheath) ($\lambda_{mfp} \gg \lambda_{De}$) which implies $\lambda_{De}/\lambda_{mfp} \ll 1$. Thus, from the Poisson's Eq. (20) it is evident that the space charge effect is weaker and hence the dynamics is governed by quasineutrality condition

$$N_e = N_i + \epsilon_I N_I. \quad (22)$$

Using the continuity Eqs. (16) and (18), the normalized momentum Eqs. (17) and (19) can be written as below,

$$M_i \frac{dM_i}{d\xi} = \frac{d\psi}{d\xi} + \frac{\gamma_i T_i}{T_e} \frac{1}{M_i} \frac{dM_i}{d\xi} - \hat{v}_{in} M_i, \quad (23)$$

$$M_I \frac{dM_I}{d\xi} = Z_I \frac{m_i}{m_I} \frac{d\psi}{d\xi} + \frac{\gamma_I T_I}{T_e} \frac{m_i}{m_I} \frac{1}{M_I} \frac{dM_I}{d\xi} + \hat{g}_E - \hat{v}_{In} M_I. \quad (24)$$

Equations (15) and (22) yield an expression for $d\psi/d\xi$ in terms of the ion and dust densities,

$$\frac{d\psi}{d\xi} = -\frac{1}{N_e} \frac{dN_e}{d\xi} = -\frac{1}{N_i + \epsilon_I N_I} \left(\frac{dN_i}{d\xi} + \epsilon_I \frac{dN_I}{d\xi} \right). \quad (25)$$

Thus, using the continuity Eqs. (16), (18) in (25), Eqs. (23) and (24) can be reduced to a pair of coupled first-order differential equations,

$$\left[\left(\frac{M_i}{M_i + \alpha M_i} + \frac{\gamma_i T_i}{T_e} \right) - M_i^2 \right] \frac{dM_i}{d\xi} - \frac{\alpha M_i^2}{M_i (M_i + \alpha M_i)} \frac{dM_d}{d\xi} = \hat{v}_{in} M_i^2, \quad (26)$$

$$- \frac{Z_I m_i}{m_I} \frac{M_I^2}{(M_I + \alpha M_I)} \frac{dM_I}{d\xi} + \left[\left(\frac{Z_I m_i}{m_I} \frac{\alpha M_i}{M_i + \alpha M_i} + \frac{\gamma_I T_I m_i}{T_e m_I} \right) - M_I^2 \right] \frac{dM_I}{d\xi} = \hat{v}_{In} M_I^2 - \hat{g}_E M_I. \quad (27)$$

B. The sheath region

In the sheath region the space charge effect dominates and thus the full Poisson's Eq. (20) is used to find solutions. A ratio L/λ_{De} appears in the right-hand side of Eq. (20). This ratio L/λ_{De} is used to account for the scale transition from a longer scale to a smaller scale to achieve smooth transition from presheath to sheath region. This gives the relative scaling of the presheath and the sheath scale and when introduced allows the Poisson's equation to be applied everywhere in the plasma to solve the discontinuity at the sheath edge.

The final set of equations to be solved on the sheath scale can be written from Eqs. (16)–(20) as

$$\left(M_i^2 - \frac{\gamma_i T_i}{T_e} \right) \frac{dM_i}{d\xi} = M_i \frac{d\psi}{d\xi} - \hat{v}_{in} M_i^2, \quad (28)$$

$$\left(M_I^2 - \frac{\gamma_I T_I}{T_e} \frac{m_i}{m_I} \right) \frac{dM_I}{d\xi} = Z_I \frac{m_i}{m_I} M_I \frac{d\psi}{d\xi} + \hat{g}_E M_I - \hat{v}_{In} M_I^2, \quad (29)$$

$$\frac{d^2\psi}{d\xi^2} = \left(\frac{L}{\lambda_{De}} \right)^2 [N_i + \epsilon_I N_I - N_e]. \quad (30)$$

The electron distribution can be written from Eq. (15) as below,

$$N_e = \exp(-\psi). \quad (31)$$

V. THE SOLUTION PROCEDURE

Usually, sheaths are investigated without considering presheaths because of the significantly different space scales of both regions as discussed above. Very often the boundary conditions are formulated using the Bohm's boundary conditions at the sheath edge. Unfortunately, Bohm's boundary conditions are not self-consistent and leads to singularities at the interface between the presheath and the sheath. However, there is a possibility to solve the presheath and sheath self-consistently without imposing specific boundary conditions

but by solving the equations in the presheath limit to determine the boundary condition at the sheath edge and applying these boundary conditions to solve the equations in the sheath limit. A similar solution procedure is adopted in this analysis and involves the following steps:

(1) In determining the solutions in the presheath region, Eqs. (26) and (27) are cast in the form of a matrix equation,

$$\begin{pmatrix} A_{11} & A_{12} \\ A_{21} & A_{22} \end{pmatrix} \begin{pmatrix} M_i' \\ M_I' \end{pmatrix} = \begin{pmatrix} b_1 \\ b_2 \end{pmatrix}, \quad (32)$$

where

$$A_{11} = \left(\frac{M_I}{M_I + \alpha M_i} + \frac{\gamma_i T_i}{T_e} \right) - M_i^2,$$

$$A_{12} = - \frac{\alpha M_i^2}{M_I (M_I + \alpha M_i)},$$

$$A_{21} = - \frac{Z_I m_i}{m_I} \frac{M_I^2}{M_i (M_I + \alpha M_i)},$$

$$A_{22} = \left(\frac{Z_I m_i}{m_I} \frac{\alpha M_i}{M_I + \alpha M_i} + \frac{\gamma_I T_I m_i}{T_e m_I} \right) - M_I^2,$$

$$b_1 = \hat{v}_{in} M_i^2,$$

$$b_2 = \hat{v}_{in} M_I^2 - \hat{g}_E M_I.$$

Then the equations to be implemented in the program are given by

$$\begin{pmatrix} M_i' \\ M_I' \end{pmatrix} = \begin{pmatrix} A_{11} & A_{12} \\ A_{21} & A_{22} \end{pmatrix}^{-1} \begin{pmatrix} b_1 \\ b_2 \end{pmatrix}. \quad (33)$$

(2) The above Eq. (33) is solved numerically. The plasma system assumed is such that the system length is much longer than the mean free path of the dust grains. Thus, the natural entry value for initial flow velocity of dust grains is the terminal flow velocity ($M_{I0} = \hat{g}_E / \hat{v}_{in}$) reached under the collective effect of external gravity and dust neutral drag. The ions enter the presheath with a small initial flow velocity.

(3) The condition $\det A = [A_{11}A_{22} - A_{12}A_{21}] = 0$ is equivalent to the Bohm singularity in this system and thus defines the position at which the quasineutrality breaks down and the sheath begins.

(4) In $(M_i - M_I)$ space, this corresponds to a curve on which $\det A = 0$. The topology of $\det A$ is explored to find solutions in different set of parameter regimes.

(5) In the sheath region the equations to be implemented are written in the form

$$\frac{dM_i}{d\xi} = - \frac{M_i}{\left[\frac{\gamma_i T_i}{T_e} - M_i^2 \right]} \frac{d\psi}{d\xi} + \frac{\hat{v}_{in} M_i^2}{\left[\frac{\gamma_i T_i}{T_e} - M_i^2 \right]}, \quad (34)$$

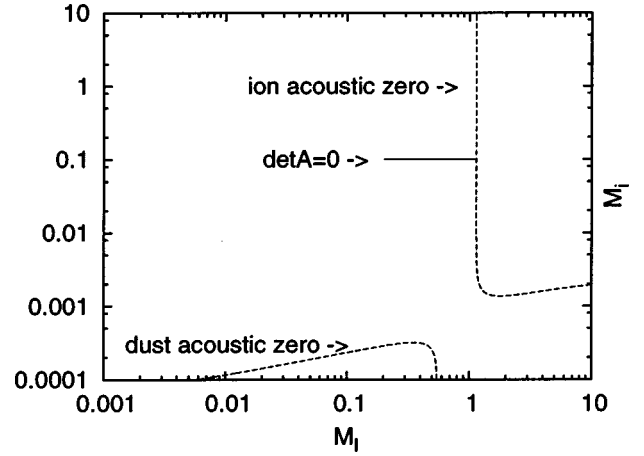


FIG. 2. Root locus of solutions for case I, where dust grains do not couple strongly to the plasma. The dashed lines indicate the ion-acoustic and dust acoustic presheath singularities. The solid line indicates the evolution of the solution in $M_i - M_I$ space for a case where the ion velocity builds up steadily till the ion acoustic zero is reached. This is the standard presheath.

$$\frac{dM_I}{d\xi} = - \frac{Z_I m_i}{m_I} \frac{M_I}{\left[\frac{\gamma_I T_I}{T_e} \frac{m_i}{m_I} - M_I^2 \right]} \frac{d\psi}{d\xi} + \frac{\hat{v}_{in} M_I^2}{\left[\frac{\gamma_I T_I}{T_e} \frac{m_i}{m_I} - M_I^2 \right]} - \frac{\hat{g}_E M_I}{\left[\frac{\gamma_I T_I}{T_e} \frac{m_i}{m_I} - M_I^2 \right]}, \quad (35)$$

$$\frac{d^2\psi}{d\xi^2} = \left(\frac{L}{\lambda_{De}} \right)^2 \left[\frac{M_{i0}}{M_i} + \epsilon_I \frac{M_{I0}}{M_I} - \exp(-\psi) \right]. \quad (36)$$

(6) In treatments of sheath region found in literature, $M=1$ is usually chosen as the boundary condition at the sheath edge with finite electric field. But this results in discontinuities and singularities of the electric field at the plasma sheath interface and thus fails to match the plasma and sheath solutions smoothly. Therefore, an alternate treatment is described in this work to solve the equations for the space charge dominated sheath region. At some point well within the presheath, the value of the electric field and flow velocity are found self-consistently from the presheath equations and using these initial conditions Poisson's equation is then solved for some finite value of $\lambda_{De} / \lambda_{mfp}$.

VI. RESULTS AND DISCUSSIONS

The equations formulated for the presheath and sheath region were implemented in a FORTRAN 77 program and adaptive-Runge-Kutta method was used to solve them for a low temperature argon plasma. Solving Eq. (33) in the presheath limit, three distinct cases of interacting and noninteracting dust grains were identified. The size and number density of dust grains determine the properties of the plasma system. A study of the topology of $\det A$ [defined in Eq. (32)] identified three cases which are plotted in Figs. 2, 3, 4. These plots present the ion and dust velocities in $M_i - M_I$ space. Each point corresponds to the solution at some $\xi = z/L$. The dashed lines in Figs. 2, 3, and 4 represent the points in

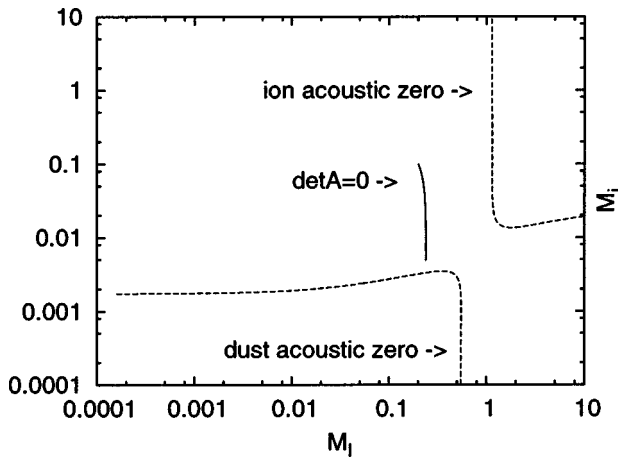


FIG. 3. Root locus of solutions for the second case where again the dust grains do not couple strongly to the plasma. The dashed line indicate the ion-acoustic and the dust-acoustic presheath singularities. The solid line indicates the evolution of the solution in M_i - M_I space for a case where the dust velocity drops till dust acoustic zero is reached. This also is the case of the standard presheath but for the dust domain.

(M_i - M_I) space corresponding to $\det A=0$. The presheath solution (solid line) must approach these dashed lines if it is to develop into a sheath near the wall.

Figure 2 shows the case for the dust grains of size 1–2 μm . The dust number density was very low as compared to the ions, i.e., $n_{I0} \approx 10^{-8} n_{i0}$. The root locus (the presheath solution) reached the ion acoustic zero (ion acoustic speed) as shown in the plot (Fig. 2).

Keeping the number density as before, if the dust grains of smaller size, i.e., $a \sim 0.1 \mu\text{m}$ were considered the root locus (the presheath solution) reached the dust acoustic zero as seen in Fig. 3. Figure 3 presents the situation for a smaller dust particle. The smaller size permits a higher terminal velocity, and the $\det A=0$ curves are also shifted. As a conse-

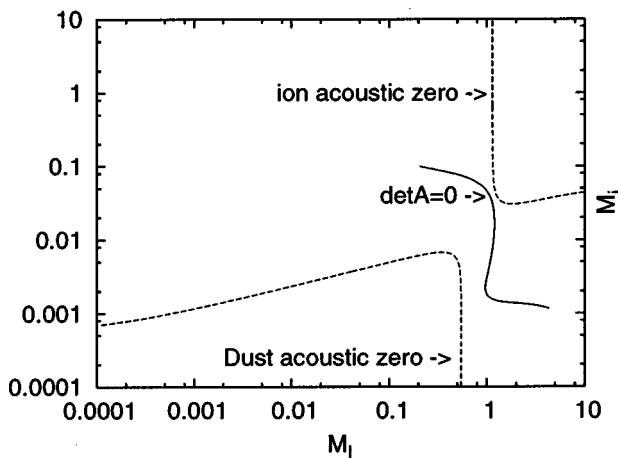


FIG. 4. Root locus of solutions for the third case where the dust grains are coupled strongly to the plasma. The dashed lines indicate the ion-acoustic and the dust-acoustic presheath singularities. The solid line indicates the evolution of the solution in M_i - M_I space for a case where the ion velocity builds up to its singular value and at the same time the dust velocity shows interesting features of stagnation towards the sheath edge.

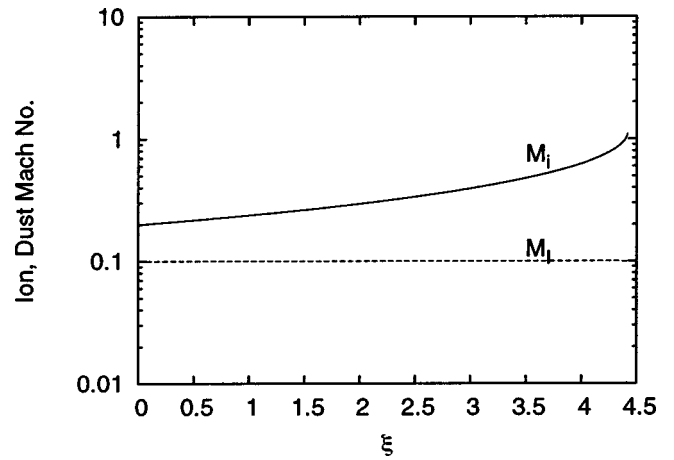


FIG. 5. Velocity profiles for the ions and dust grains in the presheath region for case I. The solid line represents the ion velocity M_i and the dashed line the dust velocity M_I . The curves are plotted on a log scale.

quence, it is found that this system evolves to the point where it intersects the dust-acoustic singularity, instead of the ion-acoustic singularity.

In the third case, a distinct and unique solution was obtained as seen in Fig. 4. This was the case when the dust number density was appreciable, $n_{I0} \approx 10^{-6} n_{i0}$ and the dust grains of size $a \sim 0.5 \mu\text{m}$ were considered. The dust grain size was in between the earlier two cases. The root locus profile showed unique features. It neither approached the ion acoustic zero nor the dust acoustic zero. It passed in between the two and then flattened.

The three cases identified above were the solutions obtained in the quasineutral regime. These three cases were then extensively studied in the whole plasma region. The equation for presheath region and the sheath region were solved in continuity. The boundary values at the sheath edge, plasma–sheath interface, were calculated self-consistently from the presheath equations. The results for the three cases are discussed below.

A. Case I

The first case considered 1–2 μm sized dust grains. The number density of dust grains was very low. The velocity profile of both ions and dust grains in the presheath region are plotted in Fig. 5. The ions which started with an initial velocity ($v_{i0} = 0.2c_s \text{ms}^{-1}$) approached the acoustic speed (c_s) at the sheath edge. The dust grains entered the presheath region with a terminal speed ($\hat{g}_E/\hat{v}_{In} = 0.1$) and remained unaffected in the whole presheath region upto the sheath edge. Due to the low number density of dust grains, the dusts do not get coupled to the plasma as clearly indicated by the unchanged velocity profile of dust grains (Fig. 5). Thus, this represents a case of noninteracting dust grains.

The point at which $\det A=0$, defines a point where the quasineutrality breaks down and the space charge dominated sheath region begins. This point is referred to as “sheath edge.” At this point the ions enter the sheath with a velocity greater than the acoustic speed, i.e., $M_{i0} > 1$, fulfilling the Bohm condition. The ions in this case fulfill the Bohm condition as clearly seen in Fig. 5.

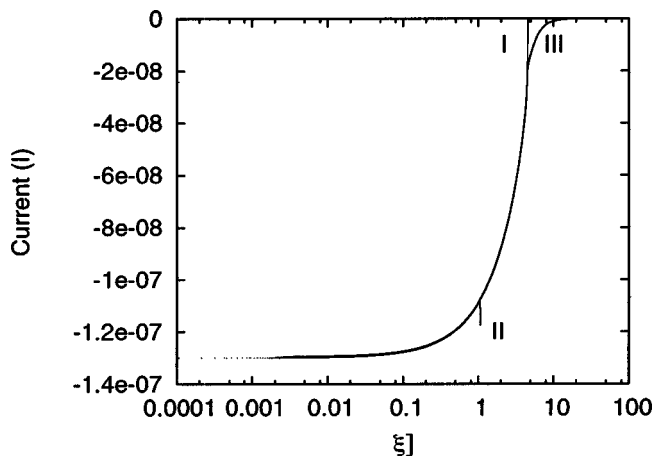


FIG. 6. The net current profiles for the three cases which include the contributions from ions, dust grains and the electrons which are reflected away from the wall is plotted vs ξ . The curves are marked I, II, III for the three distinct cases.

The dynamics of the plasma species in the whole plasma region were studied under the floating boundary wall condition. The floating sheath boundary condition at the wall, demands that zero net current is drawn by the wall, i.e., $I_e + I_i + I_d = 0$, where I_e , I_i and I_d are the electron, ion and dust currents to the wall. This boundary condition determines the position of wall. The curve marked "I" in Fig. 6 shows the profile of the total current approaching zero for case I.

Figure 7 shows the velocity profile of ions and dust grains in the whole plasma, the quasineutral presheath, and the space charge dominated sheath regions. The equations for both presheath and the sheath were solved in continuity. As described in Sec. IV, the boundary values at the sheath edge were calculated self-consistently from the presheath equations and then substituted into the Poisson Eq. (36). The Poisson's equation was then solved for a finite value of $\lambda_{De}/\lambda_{mfp}$. The standard ion acoustic sheath solution was achieved in this case. The ion velocity increased monotonically to reach the wall and the dust grain velocity remained unaffected (Fig. 7).

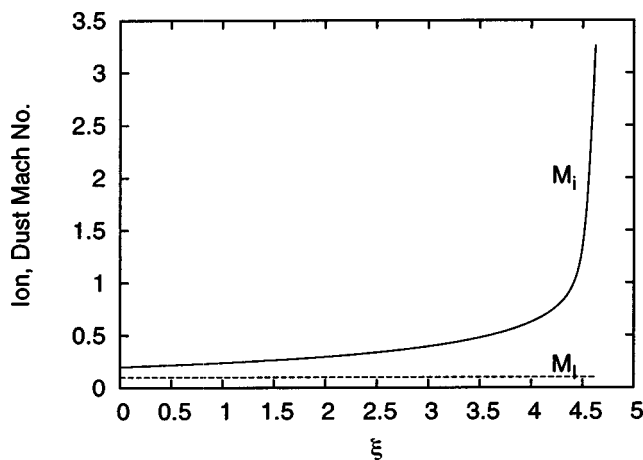


FIG. 7. Monotonic velocity profile of ions for case I. The solid curve denotes the M_i curve and the dashed curve denotes the M_d curve plotted vs ξ .

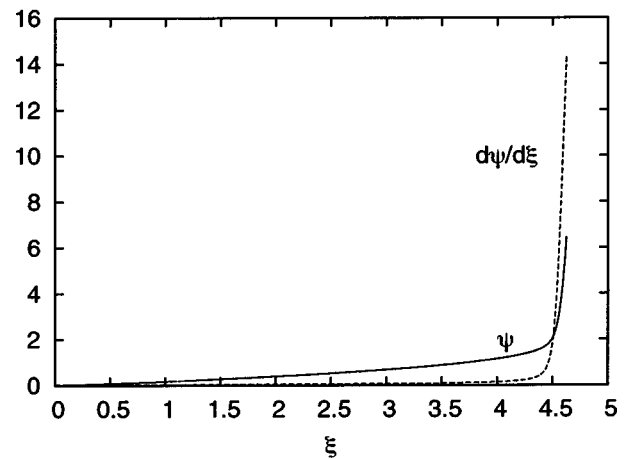


FIG. 8. Potential (ψ) and electric field ($d\psi/d\xi$) profiles for case I. ψ profile is monotonic. Electric field also show standard sheath features.

The monotonic potential profile and the electric field variation are shown in Fig. 8. The profiles were similar to the standard sheath solutions. A very small potential ψ existed in the presheath region and showed a steep rise in the sheath region. Similarly, the electric field ($d\psi/d\xi$) was almost zero in the quasineutral presheath and increased steeply in the sheath region.

The spatial variation of dust charge variation is shown in Fig. 9. Dust charge increased in the presheath region and decreased in the sheath region. The increase of dust charge in the quasineutral limit and a subsequent decrease in space charge dominated region could be explained as follows: The electron and ion currents reaching the dust grain determines the charge on the dust grains. The dust grain collects thermal electron current in the whole plasma region whereas the ion current is thermal in the low streaming velocity limit (presheath region) and streaming in the high streaming velocity limit (sheath region). In the presheath region, where quasineutrality dictates the dynamics, the ions are streaming with a low velocity. This results in the decrease of accretion radius of ions on dust surface and hence an increase in the

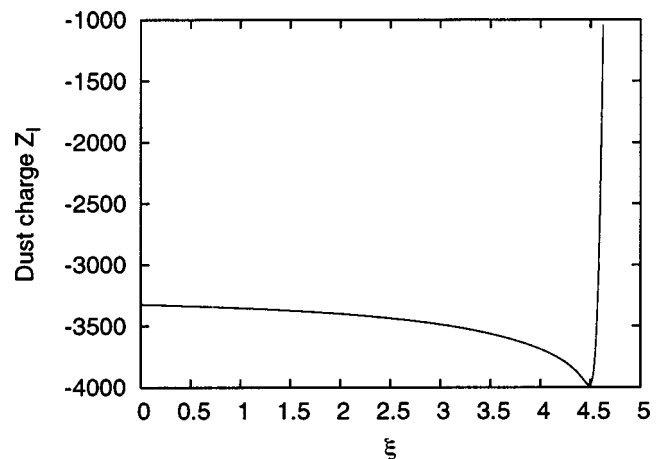


FIG. 9. Charge on dust grains Z_d plotted vs ξ for case I. The charge shows an increase in the presheath region and then a sharp decrease in the sheath region.

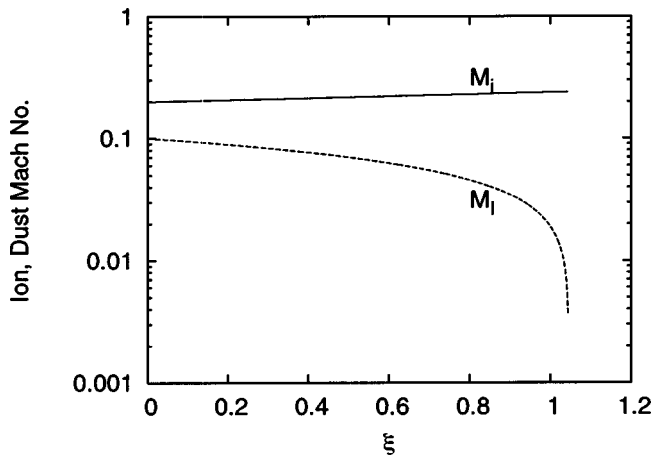


FIG. 10. Velocity profile of ions and dust grains in the presheath region for case II (plotted on a log scale). The dust grains show a drop in flow velocity (dashed curve) and ions show no appreciable change in flow velocity (solid curve).

electron accretion radius. The increase in the electron accretion radius results in the increase in the charge on the dust surface. Thus, as shown in Fig. 9 the charge on dust increased in the presheath region, the region dominated by thermal ion currents. In the sheath region where the space charge effect becomes dominant, the streaming speed of ions affect the ion current. Thus, near the sheath, the accretion of electrons decreases and ion accretion increases. The electrons are repelled by the negative potential of the wall and ion density increases as the ions stream towards the boundary wall. This results in the decrease of charge on dust grains as shown in Fig. 9.

B. Case II

Keeping the number density of dust grains same as in case I, ($n_{i0} = n_{i0} 10^{-8}$), the dust grains of smaller size, $a \sim 0.1 \mu\text{m}$, were introduced in the plasma and the solutions in the dust domain were obtained. Since the number density was very small in this case also, the dust grains remained uncoupled and the solutions for noninteracting dust grains were obtained. In this case the dust dynamics dominated and the presheath solutions for dust regime were obtained. The velocity profiles in the presheath region for the ions and dust grains on logscales are shown in Fig. 10. The dust grain flow velocity dropped to a singular value ($\sim c_{sI}$ the acoustic speed of dust grains) at the sheath edge whereas the ion flow speed showed no appreciable change. The standard presheath solution was reached in this case also but for the dust domain.

The solutions for the whole plasma, the presheath and the sheath, were obtained using the same procedure as in case I. The velocity profiles in the whole plasma are shown in Fig. 11. The dust grain flow velocity dropped further and then showed a steep rise whereas the ion flow velocity shoots up steeply. The density profile for the ions and dust grains is shown in Fig. 12. A steep structure is formed for the dust grains whereas the ion number density drops steeply in the sheath region.

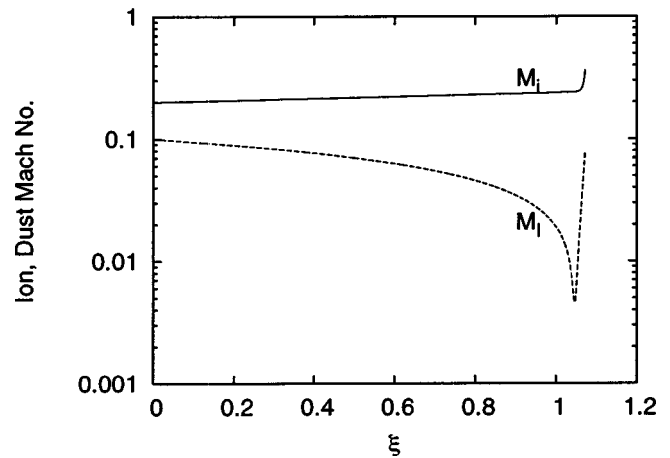


FIG. 11. Velocity profile of ions and dust grains for case II in the whole plasma.

This case, though presented a distinct solution, was numerically unstable. The zero net current condition which need to be satisfied to reach the wall was not achieved in this case (curve marked II in Fig. 6). The program terminated well before the boundary wall (sheath) was reached. The direction of the total current was reversed. The potential and electric field also showed sign reversal as shown in Fig. 13. Physically the results could be interpreted as follows. Flux conservation demands that the drop in the velocity of dust grains should result in the increase in the density of dust grains. This increase in the number density of dust grains results in the formation of a dust cloud. This cloud acts as a virtual nonlinear potential structure, a pseudosheath. The ions get accelerated towards the dust cloud under the affect of the potential structure. Thus, the formation of dust cloud reduces the electron and ion currents reaching the wall as it diverts the electrons and the ions away from wall. This results in the reorganization of the sheath potential (sign reversal of the potential, Fig. 13). The reorganization of the sheath potential in turn affects the dust cloud. The sign reversal of potential act as a potential well for the negative dusts and

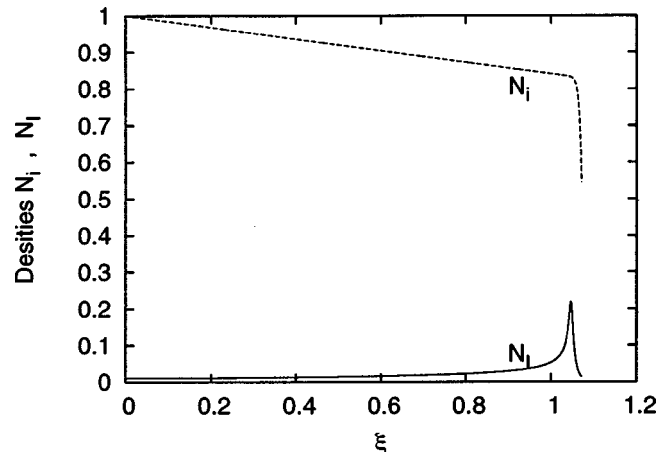


FIG. 12. Density profile of ions and dust grains in the whole plasma for case II. The dust density shows the formation of a steep structure as the dust slows down. Dust values are raised by an order 10^8 to plot it together with ion plot.

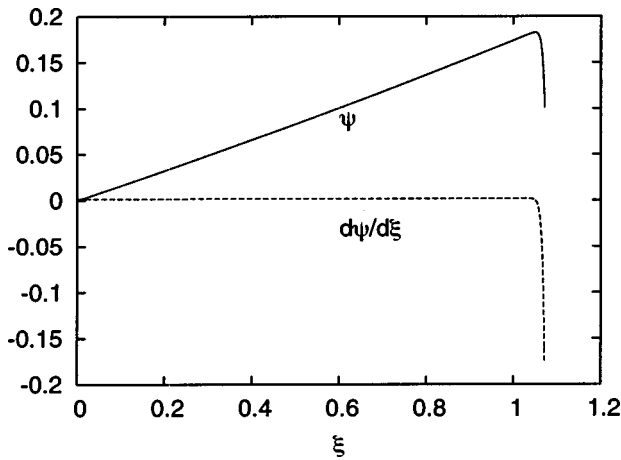


FIG. 13. Potential and electric field shows a sign reversal in case II.

thus breaks up the dust cloud. The breaking up results in the flow of dusts towards the wall along with the ions. The solutions obtained needs further improvement in the light of the unstable numerical behavior.

C. Case III

This case was solved for the parameters $n_{I0} = 10^{-6} n_{i0}$ and $a \sim 0.5 \mu\text{m}$. This case presented a distinct case as the solutions for the other limit, i.e., the interacting dust grain limit were obtained. The dust grains get coupled with the electrons and ions and affect the dynamics of sheath formation. The velocity profile for ions and dust grains is shown in Fig. 14. The presheath solution in Fig. 4 presented a unique and distinct feature which could also be observed in the curves in Fig. 14. Both ions and dust grains show unique profiles. The uniqueness of this case lies in the fact that the net current approached zero in the quasineutral region itself (curve marked III in Fig. 6). Thus, in this case, the floating wall condition was reached in the presheath limit itself and the Poisson term became redundant.

The curves in Fig. 14 shows the velocity profile of ions and dust grains. The dusts entered the presheath with a ter-

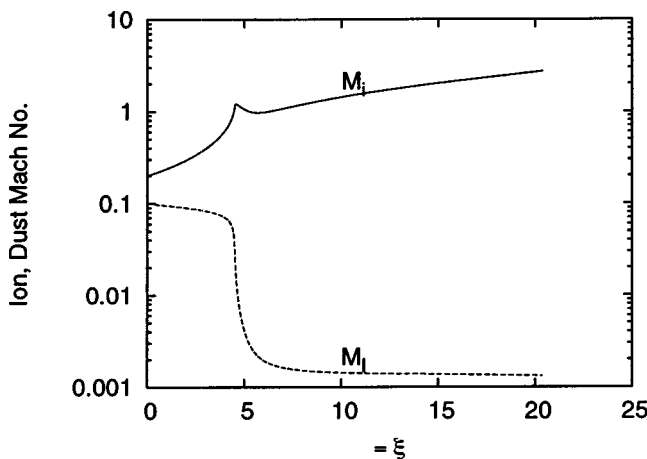


FIG. 14. Velocity profile of ions and dust grains for case III. The ions profile (solid curve) shows a kink at the point when the dust velocity (dashed curve) drops sharply. The dust flow flattens as it reaches the wall.

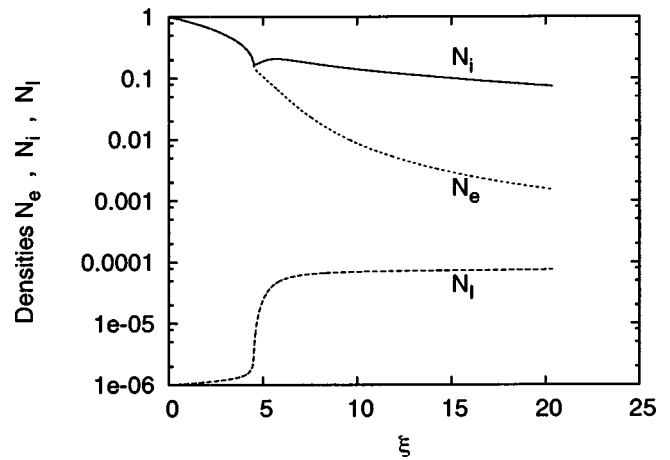
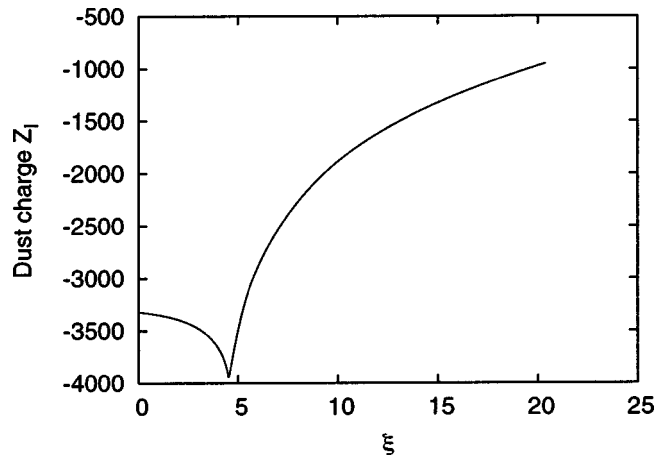


FIG. 15. Density profiles of electrons, ions, and dust grains for case III. The dust density rises, the electrons density drops faster than the ion density.

minial velocity $M_{I0} = \hat{g}_E / \hat{v}_{In} = 0.1$ and ions with an initial velocity $M_{i0} = 0.2$. Near the sheath edge the electrostatic potential of sheath affect the dynamics of plasma particles. The dust velocity dropped to a minimum and then stagnated to a new terminal flow velocity. The ion velocity increased monotonically towards the sheath. At the point where the dust velocity dropped to a minimum, the ion velocity attained the acoustic limit $M_i > 1$. A kink in the ion profile was seen at this point and then a steady increase till the zero net current condition was achieved.

The curves in Fig. 14 could be explained as follows. Combined effect of gravity, neutral drag, and electrostatic potential controls the dynamics of the dust grains. Gravity accelerates the grains while the neutral drag and the electrostatic potential resist the flow of the grains. The balance of gravity and neutral drag forces determines the terminal flow \hat{g}_E / \hat{v}_{In} with which the dust grains enter the presheath. The grains fall through the presheath with this terminal flow velocity until it experiences a resistive force due to the electrostatic potential. When the electrostatic potential becomes dominant (near the sheath edge) it resists the flow of dust grains which results in the drop in the dust flow velocity to a minimum. Thus, under the combined effect of gravity, neutral drag, and electrostatic potential the dust grains flow with a new terminal flow velocity towards the wall. This new terminal flow velocity is equivalent to the acoustic speed of dust grains defined by $c_{sI} = Z_I \sqrt{(n_{I0} / n_{i0}) (T_i / m_I)}$. The flattening of dust profile signifies the balancing of forces in this region. From flux conservation, the drop in dust velocity implies a rise in the dust number density. This could be seen in the density profiles in Fig. 15. The increased number density (dashed curve) could be related to the experimental observation of accumulation of dust grains, commonly known as trapping, near the boundary wall or surfaces.^{3,5,17} Thus, the balancing of forces could be the cause of accumulation or trapping of dust grains near the boundary wall (sheath). The trapping of dust reorganizes the conventional plasma sheath profile to a new equilibrium profile, the levitational equilibrium, where the usual sheath disappears and the trapped dust grains acts as a virtual negative

FIG. 16. Charge on dust plotted vs ξ for case III.

wall for the plasma. The ions, on the other hand, are accelerated monotonically towards the negative potential of the wall. The ions experience a shift in the potential due to the trapping of dust grains. The reorganization of the sheath structure appears as a kink in the velocity profile of ions, which signifies that the ions are accelerated under the effect of new potential structure formed due to dust trapping.

The density profile of electrons, ions and dust grains is shown in Fig. 15. The dust grains stagnate near the wall under the force balancing condition. The dust number density shows a steep rise in this region. In the standard sheath solution the electrons are repelled by the negative wall and thus the electron density thus falls faster than the ion density. But in this case the ion density falls faster than the electron density which could be attributed to the reorganization of the sheath equilibrium to a new equilibrium. Due to high dust density near the wall, a finite electron density is needed to maintain the charge on the dust grains.

The charge variation of dust is shown in Fig. 16. The dust charge showed an initial increase and this can again be explained by the previous arguments of the decrease in the accretion radius of ions as compared to the electrons. The dust charge showed a decrease at the point when the dust flow stagnated. One of the possible reasons for the decrease in the dust charge could be due to the reduction in the electron density in the sheath region. The charge on the dust grain is calculated under the isolated dust grain approximation, $a \ll \lambda_D \ll d$, where d is the intergrain distance, a is the size of grain, and λ_D is the Debye length. It is obvious that as the dust number density N_I increases, the intergrain distance may drop below the shielding distance and the grains start to interact electrostatically. For such a case one has to consider the nonisolated dust grains, instead of isolated dust grains. For nonisolated dust grains, the charge on the dust grains not only depend on the radius of grains, but also on the dust particle number density N_I . For a nonisolated case an increase in the dust particle number density means that the dust grains have a large appetite for the electrons, but the number of available electrons per dust grain decreases. Thus, when the dust number density increases as shown by the dashed curve in Fig. 16, the charge on the grains reduces.

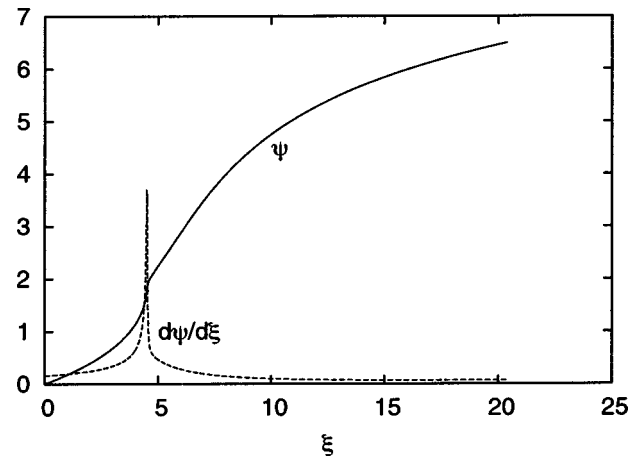


FIG. 17. Nonmonotonic potential profile for case III. Electric field profile shows the formation of a nonlinear structure.

Thus, there exists a possibility of transition from the limit of isolated dust grains to the nonisolated dust grains. This will however need further investigation for better understanding, which is not possible under the considered model and will be taken as the future course of work.

The presence of dust reorganized the plasma sheath potential and the electric field as plotted in Fig. 17. Both show a nonmonotonic behavior. A spiky structure appears in the electric field profile. Thus, the local reshuffling of the presheath potential profile under the collective effect of gravity, neutral drag, and electrostatic potential of sheath introduces a new equilibrium profile of sheath. This new equilibrium achieved gives the signature of a levitational kind of equilibrium profile that joins the presheath to the wall. The solutions presented in case III are unique in itself, since the Poisson's equation became insignificant in this case. The whole solutions were mapped on the quasineutral region itself.

VII. CONCLUSIONS

A gravitationally sensitive colloidal plasma was analyzed numerically. The results presented in the above section discussed in detail how the presence of massive dust grains modified the flow structures of plasma species in the presheath region as well as the sheath region. The boundary conditions were also modified due to the presence of dust grains. The smooth transition achieved from one region to another and the complete solutions obtained in the whole plasma region was a novel treatment in itself.

The analysis presents two situations of interest: (i) the dust particles do not affect significantly the properties of the plasma they are embedded in (this usually corresponds to low number density of the dust component, i.e., to a lower number of dust particles), and (ii) the dust component is relatively dense, thus changing significantly the field and density distributions of the surrounding plasma. Under the above mentioned situations three distinct solutions were identified for three different sets of size and number density of dust grains. For a low number density case, i.e., $n_{I0} = 10^{-8} n_{i0}$ and $1-2 \mu\text{m}$ size grains, the standard sheath so-

lutions were obtained. At low densities, we have fewer than one dust grain per Debye sphere. Thus collective modes mediated by dust such as the dust-acoustic mode are not sustainable. Such systems are very collisional, and quickly achieve their thermodynamic steady states. In dc analysis therefore, it is still reasonable to model the dust grains as a fluid as done in this paper. Keeping the dust number density same, if the dust grains of smaller size, $\sim 0.1 \mu\text{m}$, were introduced in the plasma the solutions in the dust domain were obtained. This case needs further attention in order to solve the discrepancy to arrive at the zero net current condition and treat the numerical unstable behavior. Both these solutions were for the cases when the dust grains do not couple with the plasma. The third case is the distinct case. This is for parameters $n_{i0} = 10^{-6} n_{i0}$ and size $0.5 \mu\text{m}$. The dusts get coupled to the plasma and present unique solutions. The Poisson term became insignificant in this case as the net current goes to zero in the presheath limit itself. The signature of levitational equilibrium was seen which results in the trapping of dust grains near the wall as observed experimentally by many investigators.^{6,17}

The coupling between the gravitational force and neutral drag force defines the initial flow condition for dust grains. The collective dynamics of gravitational force, electrostatic force of sheath, and neutral drag force results in a flattening of dust profiles for the third case. This flattening of dust flow could be attributed to the levitation of dust grains achieved due to force balancing. This could be related to the “particle trap”³ as observed and discussed in experiments. The flattening in the dust flow profile is reached due to balancing of various forces and it can be the signature of the quasilevitational kind of equilibrium²⁴ at the interface between the presheath and the Debye sheath. The dust grains flow with a new terminal speed of the order of acoustic speed of dust (c_{st}) in this equilibrium zone. The term “quasi” could be attributed to the finite dust speed of the order of dust acoustic speed with which the dusts reach the wall. The situation when the dust grains couple strongly with the plasma corresponds to interesting self-organized dust plasma structures such as crystals, clouds, voids, etc., which are observed in the vicinity of the sheath. The results discussed above could be useful in explaining some facts related to the formation of these structures near the sheath.

ACKNOWLEDGMENTS

One of the authors (K.R.R.) would like to thank Council of Scientific and Industrial Research, India, for the financial support to carry out this work. K.R.R. would also like to thank the Plasma Science Society of India, Institute for Plasma Research and IIT Madras, India, for providing facilities to carry out this work in collaboration with Dr. H. Ramchandran.

- ¹M. S. Sodha and S. Guha, *Advances in Plasma Physics* (Wiley, New York, 1971), Vol. 4, p. 219.
- ²P. K. Shukla, *Phys. Plasmas* **8**, 1791 (2001).
- ³G. Selwyn, G. E. Heidenreich, and K. Haller, *Appl. Phys. Lett.* **57**, 1867 (1990).
- ⁴J. F. O’Hanlon, K. Jungwon, L. K. Russell, and L. Hong, *IEEE Trans. Plasma Sci.* **22**, 122 (1994).
- ⁵A. V. Gurvich and L. P. Pitaevsky, *Prog. Aerosp. Sci.* **16**, 227 (1975).
- ⁶G. S. Selwyn, *J. Vac. Sci. Technol. B* **9**, 3487 (1991).
- ⁷B. Lipshulz, *J. Nucl. Mater.* **145**, 15 (1982).
- ⁸J. Winter, *Plasma Phys. Controlled Fusion* **40**, 1201 (1998).
- ⁹T. G. Northrop and J. R. Hill, *Geophys. Res.* **88**, 1 (1983).
- ¹⁰E. C. Whipple, T. G. Northrop, and D. A. Mendis, *J. Geophys. Res.* **90**, 7405 (1985).
- ¹¹J. H. Chu and I. Lin, *Phys. Rev. Lett.* **72**, 4009 (1994).
- ¹²H. M. Thomas, G. E. Morfill, and V. Demmel, *Phys. Rev. Lett.* **73**, 652 (1994).
- ¹³G. S. Selwyn, J. Singh, and R. S. Bennett, *J. Vac. Sci. Technol. A* **7**, 2758 (1989).
- ¹⁴J. F. O’Hanlon, *J. Vac. Sci. Technol. A* **7**, 2500 (1989).
- ¹⁵K. G. Spears, T. J. Robinson, and R. M. Roth, *IEEE Trans. Plasma Sci.* **14**, 179 (1986).
- ¹⁶G. S. Selwyn, J. S. McKillop, K. L. Haller, and B. P. Wu, *J. Vac. Sci. Technol. A* **8**, 1726 (1990).
- ¹⁷D. Winkse and M. E. Jones, *IEEE Trans. Plasma Sci.* **24**, 454 (1994).
- ¹⁸M. S. Barnes, J. H. Kellar, J. C. Forster, J. A. O’Neill, and D. K. Coultas, *Phys. Rev. Lett.* **68**, 313 (1992).
- ¹⁹J. X. Ma and M. Y. Yu, *Phys. Plasmas* **2**, 1343 (1995).
- ²⁰J. X. Ma, J. Y. Liu, and M. Y. Yu, *Phys. Rev. E* **55**, 4627 (1997).
- ²¹T. Nitter, T. K. Aslaksen, F. Melandso, and O. Havnes, *IEEE Trans. Plasma Sci.* **22**, 159 (1994).
- ²²J. Y. Liu, D. Wang, T. C. Ma, Y. Gong, Q. Sun, J. X. Ma, and C. X. Yu, *Phys. Plasmas* **6**, 1405 (1999).
- ²³F. F. Chen, in *Plasma Diagnostics Techniques*, edited by R. H. Huddleston and S. L. Leonard (Academic, New York, 1965), Chap. 4.
- ²⁴K. R. Rajkhowa, C. B. Dwivedi, and S. Bujarbarua, *Pramana, J. Phys.* **52**, 293 (1999).